Dissertation Prospectus
for
Eric J. Hunter

Department of Speech Pathology and Audiology
The University of Iowa
Iowa City, IA

Thesis Question: *To what degree can a three-dimensional biomechanical vocal fold model predict the dynamics of a posturing gesture?*

Specific Aims

1. To use existing *in vitro* data of vocal folds from laryngeal specimens to quantify the tissue geometry as well as the mechanical properties of vocal folds, including the arytenoid cartilages;
2. To develop the constitutive and dynamical equations of laryngeal posturing;
3. To define boundary conditions and utilize a FEM package to develop a three-dimensional finite-element model for a numerical solution to the equations;
4. To observe vocal fold posturing with high-speed video endoscopy for five specific laryngeal gestures on five human subjects;
5. To predict the muscle activities and coordination needed to simulate the selected gestures and motions of endoscopic high-speed video imaging; and
6. To interpret the differences between the motion of the model and the endoscopic imaging as well as to interpret the predicted muscle activations.

1. *To use existing in vitro data of vocal folds from laryngeal specimens to quantify the tissue geometry as well as the mechanical properties of vocal folds, including the arytenoid cartilages.*

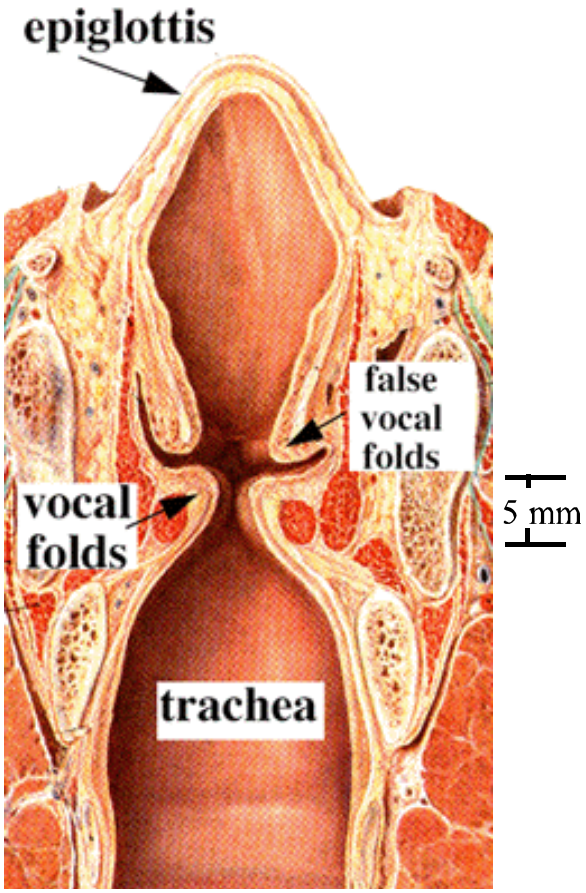

Figure 1. Coronal cross-sectional view of the larynx.

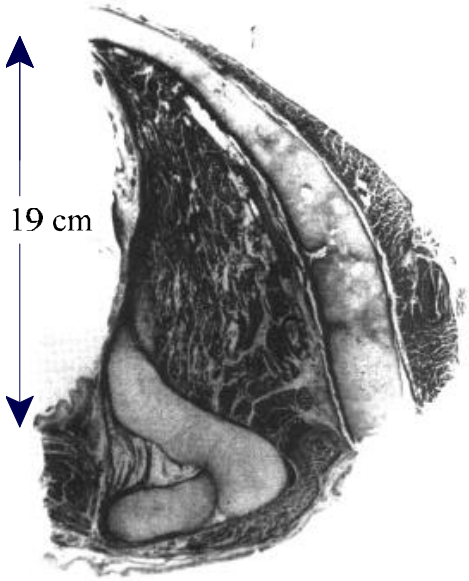

Right fold histological section.

Tissue	μ (Shear Modulus)
Cartilage	$1x10^6$ Pa
Soft Tissue	$1x10^2$ Pa

2. *To develop the constitutive and dynamical equations of laryngeal posturing.*

Hooke's Law, a linear constitutive equation is

$$ó = E å , \qquad E = \mu(1 + í) , \tag{1}$$

Constants	Definitions
Young's Modulus (*E*)	A measure of a material's stiffness
Poisson's Ratio (*v*)	A measure of a material's compressibility
Shear Modulus (μ)	A constant representing the deformation of a material when subject to a shear force

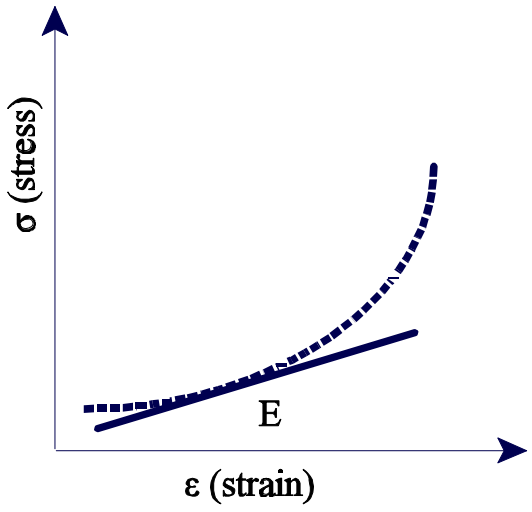

Figure. Young's Moduls.

3. To define boundary conditions and utilize a FEM package to develop a three-dimensional finite-element model for a numerical solution to the equations.

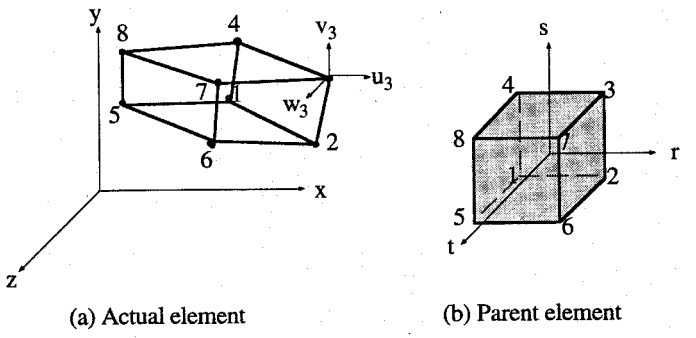

Figure 26. An eight node hexahedral (brick) element. (a) actual element. (b) parent element (mapped from actual domain).

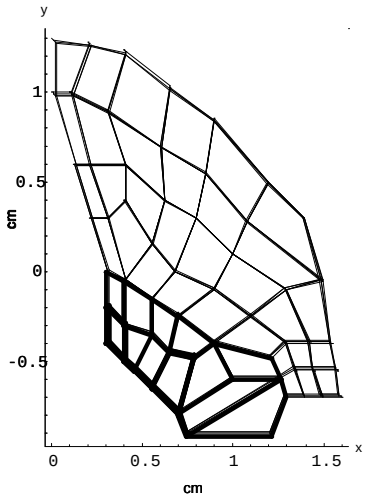

Figure 19. Simplified transverse view of the right vocal fold for FEM modeling.

Muscle	act. ó$_{max}$	direction cosines -->	x	y
TA	1x10^6 Pa		0.015	0.990

Translational Stiffness	k_x	k_y
	91 N/m	254 N/m

Results of TA contraction:
The Proposed Extension:

A. Expand the model to better illustrate the rostra-caudal direction (Figure 9):

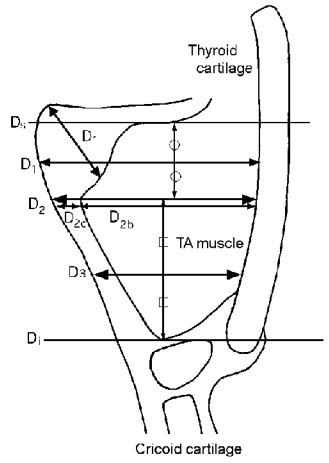

Figure 9. Coronal cross-section of the right vocal fold. Depth measures from Tayama, et al, (1999).

B. Subdivide the vocal tissue into three categories with linear material constants as in Table 2 of Chapter 2:

Table 2. Shear modulus for the three tissue types assumed in the model.

Tissue	μ (Shear Modulus)
Ligament	$2x10^4$ Pa
Cartilage	$1x10^6$ Pa
Soft Tissue	$1x10^2$ Pa

C. Allow for non-linear constitutive equations by using multiple Young's Moduli. ANSYS has this option with up to 10 values entered using a Modified Newton-Raphson Method. Or, allow all tissue to be a linear isotropic tissue with active and passive forces fed in from the

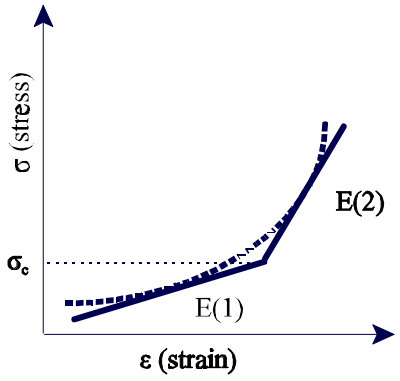

Figure. Multiple Young's Moduli for large deformations.

tissue models. Or, treat the ligament at isotropic with a non-linear Young's modulus depicted from the tissue model with the muscle a transversely isotropic material; linear perpendicular to the fibers and non-linear parallel to the fibers with the *E*'s from an average stretch from the model.

D. Add the CAJ stiffness will be modeled to allow (1) a rocking condition, (2) a sliding condition, and (3) a rotational (or twisting) condition.

i. The rocking condition will be modeled using a line of points along the base of the arytenoids, which will be constrained in the vertical position. This line of nodes will be in the direction of a rocking axis (Neuman et al, 1994; Sellars and Vaughan, 1983).

ii. The sliding condition will be modeled as a translation or motion in the horizontal plane by allowing a translational stiffness to representing the joint connective tissues.

iii. The third boundary condition, a rotational stiffness, will be modeled about the plane of translation. Rotation about a nearly perpendicular axis from the horizon has been described (Sellars and Vaughan, 1983).

These three conditions will allow the arytenoid cartilage to translate with some rotation and tip around the line of vertically constrained nodes as reported (Frabel, 1961; Negus, 1949; Von Leden & Moore, 1961; Ardan & Kemp, 1966; Fink, 1975).

Berry et al (1999) measured the translational and rotational stiffness of the CAJ associated with planar movement, with intrinsic soft tissue attached, to be nearly linear.

Translational Stiffness	k_x (N/m)	k_y (N/m)	$k_{\grave{e}}$ (Nm/rad)
	91	254	0.0120

The model will be stimulated without translational joint stiffness. An effective translational tissue stiffness provided by the tissue will be calculated. The connective tissue stiffness can be calculated by subtracting these two. The rotational stiffness associated with the connective tissue will be found in similar manner. The rotational and translational stiffnesses associated only with the joint, and not the tissue, can then be applied to the joint boundary.

E. The CTJ addition will be based on Equation 5 of Chapter 1 (Titze et al, 1988).

$$\text{å} = G(R\ a_{ct} + a_{ta}) + \text{å}_o \ ,$$

where *R*, gain of elongation, and *G*, mechanical advantage the CT has over the TA (Figure 14).

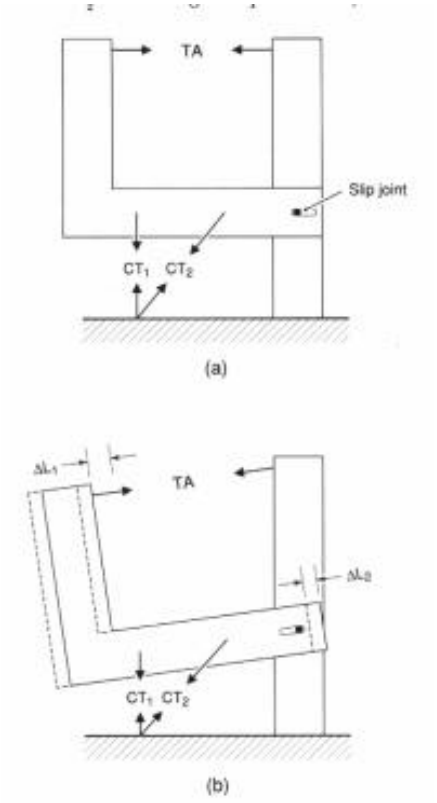

Figure 14. Crycothyroid joint mechanics schematic.

F. Use higher order elements like the twenty node isoparametric element (SOLID45 in ANSYS) as shown in Figure 28.

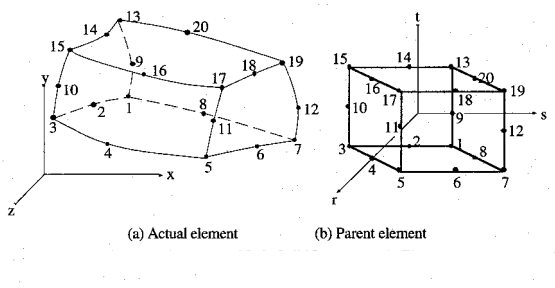

Figure 28. A twenty node isoparametric solid element. (a) actual element. (b) parent element (mapped from actual domain).

G. Use three-dimensional direction cosines for the intrinsic muscles as shown in Figure 10 (Mineck, et al, 1999). Forces will be applied simulating muscle tissue as in Figure 40.

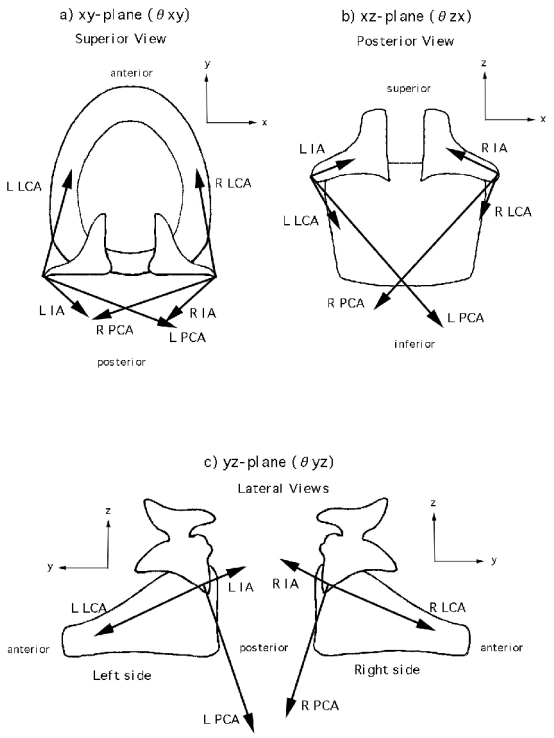

Figure 10. Resultant contraction vectors of LCA, PCA and IA muscles: (a) superior view, (b) posterior view, (c) lateral view.

H. Find all the material properties of a muscle through muscle modeling (Figure 33) from Equations 2-6 of Chapter 3 (See Figures 35-38).

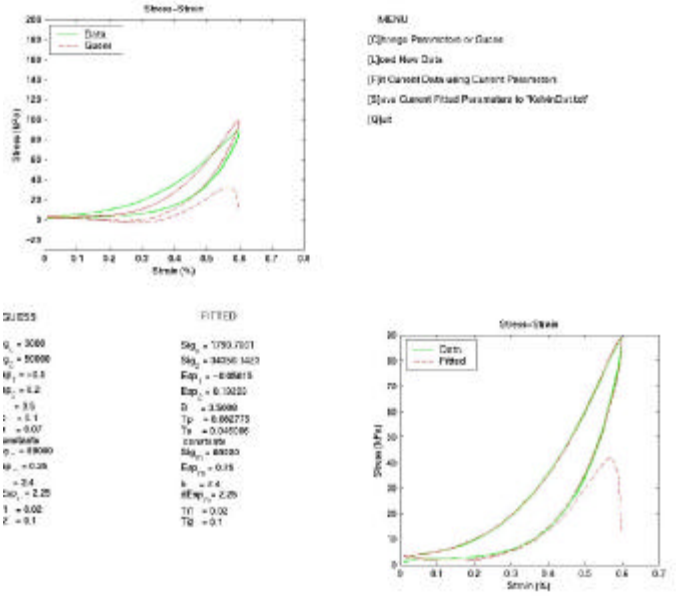

Fiigure 33. A program to fit the passive parameters of a muscle.

I. Given a strain of the TA muscle for a given position, calculate the new active stress using the muscle model equations.

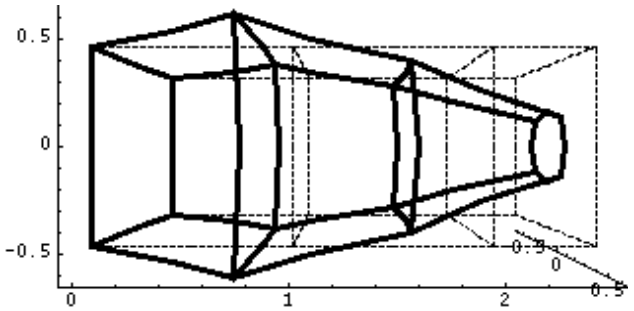

Figure 40. Three 20-node element structure. The left most element is a contractile element. Nodes were globally fixed on the left boundary. The right most boundary only has a left-right translation fixed boundary.

4. To refine and validate the model with *in vitro* dynamics (passive mechanics): the angles, strains, and speeds of an excised larynx by allowing the model's geometrical and mechanical properties to vary within one standard deviation of their original measurements;
4. *To fine-tune and validate the model with in vitro dynamics (passive mechanics); angles, strains, and speeds, of an excised larynx by allowing the model's geometrical and mechanical properties to vary within one standard deviation of original measurements.*

Make a table of all parameters used in the model... Geometry, muscle area, muscle direction, etc. Give standard deviation of original measure, etc. Adjust these measures within one standard deviation of the average until the model matches the outcome of passive motion from a laboratory setup, similar to Berry CAJ paper.

4. To observe vocal fold posturing with high-speed video endoscopy for five specific laryngeal gestures on five human subjects;

Maximum Postures

Posture	Assumed Muscle Activity
A quick sniff or inhalation (quick, maximum opening) (sniff-/i/-sniff-/i/)	the PCA will be assumed at maximum activity
A low-to-high pitch glide (fold lengthening in non-falsetto register)	CT and TA are both nearly maximum for a high pitch if the vibration is not considered a falsetto register (Titze, Luschei, and Hirano, 1989)
alternating low and high pitches	Sundberg, J. (1977), Sundberg, J. (1987).
Pressed Phonation, Cough	
A valsalva (a hard closure)	the LCA and IA will be assumed maximum

Videoscoping via laryngoscope can videotape the motions of the glottis superglottaly. Available to the investigators is a Kay Elemetrics Rhino-Laryngeal Stroboscope, Model 9100.

Time Duration of a posture will be measured. The videotaped images are recorded at 30 frames per second (Figure 31).

Glottal angle and length change can be measured for each frame.

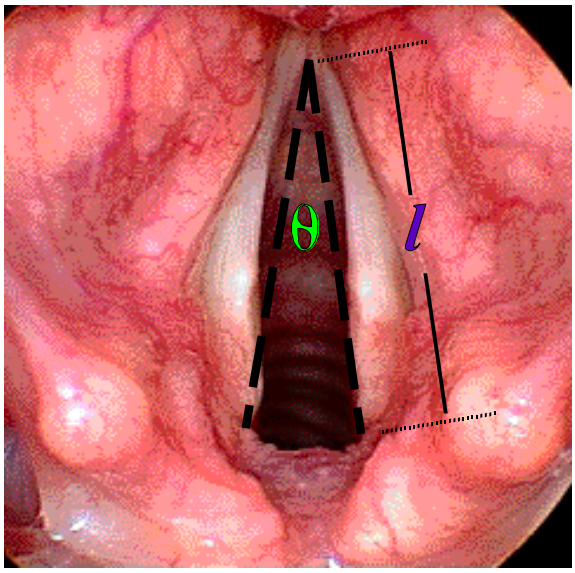

Figure 29. A relaxed glottis. Glottal angle (è) and relative glottal legnth (*l*) are depicted.

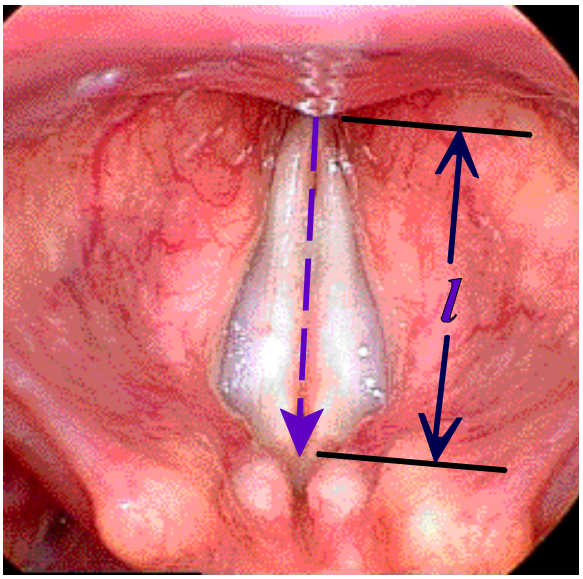

Figure 30. A closed glottis. Glottal angle (è) is zero. Relative glottal legnth (*l*) are depicted.

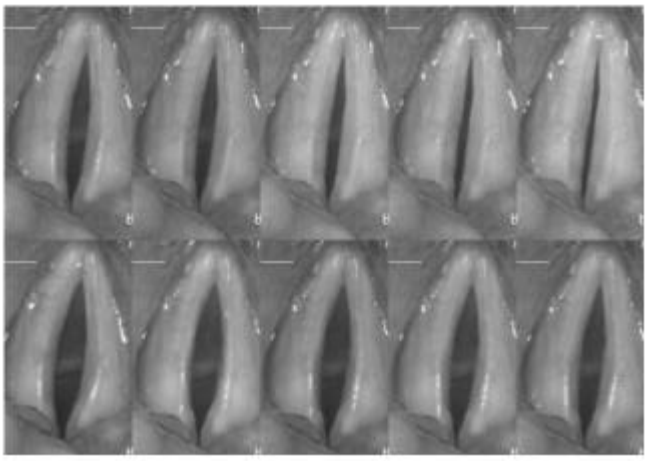

Figure 31. Stroboscopic data of vibration in a time sequence.

Dynamical Quantities (Averages)

Name	Symbol	Calculation
Glottal Angle	è	
Range of Glottal Angle	Äè	$(è_2 - è_1)/2$
Glottal Angle Rate of Change	Äè/Ät	$(è_2 - è_1)/(2\ Ät)$
Vocal Fold Length Change	Ý	$(l-l_o)/l_o$
Vocal Fold Length Rate of Change	ÝÄt	$(l-l_o)/(l_o\ Ät)$

5. To predict the muscle activities and coordination needed to simulate the selected gestures and motions of endoscopic high-speed video imaging; and
6. To interpret the differences between the motion of the model and the endoscopic imaging as well as to interpret the predicted muscle activations.

everything within a standard deviation. Make a table that has all of the parameters for the model, their averages and standard deviations.

The model will be deemed a successful representation of posturing if:

1. the same range of motion can be simulated regardless at a found muscle activity (not necessarily maximum);

2. the muscle activities, passive material constants, as well as other aspects of the model can be adjusted within a standard deviation of their laboratory measures; and

3. the resulting dynamics match the measured dynamics within a margin of **30** percent.

Dynamic information from the model and from videoendoscopy will be statistically compared for degree of similarity. When comparing the data, the following questions will be asked:

1. For what range does the model accurately depict the extent of laryngeal motion (i.e. For small strains? For large strains? Is it a linear depiction?)?; and
2. For what range does the model depict the time course of motion?